Recently observed charge radius anomaly in neon isotopes

A. Bhagwat and Y. K. Gambhir*
Department of Physics, IIT Powai, Bombay 400076, India
(Received 13 June 2003; published 8 October 2003)

The recent isotopic shift measurements for the chain of neon isotopes have revealed a rich structural information and very interesting anomalous behavior of the charge radii with neutron number. Here we study the systematics of the charge radii of neon isotopes within the relativistic mean field (RMF) framework. The pairing correlations are incorporated by simple constant gap approximation as well as self-consistently through the Bogoliubov transforms employing in the pairing channel the finite range Gogny-D1S or the density dependent zero range interaction. It is observed that the RMF in the axially deformed oscillator basis successfully explains the observed anomaly in the charge radii of neon isotopes.

DOI: 10.1103/PhysRevC.68.044301 PACS number(s): 21.10.Dr, 21.10.Ft, 21.10.Gv, 21.60.−n

The recent isotopic shift measurements for neon isotopes [1] reveal anomalous behavior and rich structure. The minimum charge radius is observed for ^{24}Ne and it rises with the addition or removal of neutrons from ^{24}Ne. The maximum radius occurs at ^{28}Ne (^{17}Ne) for neutron rich (deficient) isotopes. The neutron rich as well as deficient neon isotopes indicate a small odd-even staggering in charge radii. Further, there is a sudden drop and rise in the charge radius while moving from ^{19}Ne to ^{17}Ne. Therefore, it is worthwhile to investigate these observations theoretically. The relativistic mean field (RMF) has been successful in describing the observed anomalous behavior in the isotopic shift measurements for several nuclei in the medium (Kr, Sr, etc.) and the heavy mass regions (Rb, Gd, etc.). Therefore, it is interesting to check whether RMF will be able to describe this interesting and unusual behavior for the neon isotopes.

RMF describes the Dirac spinor nucleons interacting via the electromagnetic (e.m.) and meson fields. The mesons considered are the scalar sigma (σ), vector omega (ω), and isovector vector rho (ρ). The corresponding Lagrangian consists of free baryon and meson terms and the interaction terms. Many versions of such a Lagrangian are available. We use the standard nonlinear (σ,ω,ρ) interaction Lagrangian developed for and widely used in the nuclear structure applications [2,3]. The variational principle yields the equations of motion. In the mean field approximation, replacing the fields by their expectation values, one ends up with a set of coupled equations; namely, the Dirac equation with potential terms involving meson and e.m. fields describing the nucleon dynamics and a set of Klein-Gordon-type equations with sources involving nucleonic currents and densities, for mesons and the photon. This set of equations, known as RMF equations, is to be solved self-consistently.

The pairing correlations, essential for the description of open shell nuclei, can be incorporated either by simple BCS prescription, or self-consistently through the Bogoliubov transformations. The latter lead on to the relativistic Hartree Bogoliubov (RHB) equations. The RHB equations [3,4] read as

$$\begin{pmatrix} h_D - \lambda & \hat{\Delta} \\ -\hat{\Delta}^* & -h_D^* + \lambda \end{pmatrix} \begin{pmatrix} U \\ V \end{pmatrix}_k = E_k \begin{pmatrix} U \\ V \end{pmatrix}_k . \tag{1}$$

Here, λ is the Lagrange multiplier, E_k is the quasiparticle energy, U_k and V_k are properly normalized four-dimensional Dirac spinors, and h_D is the usual Dirac Hamiltonian [3]:

$$h_D = -\iota\alpha\cdot\nabla + \beta(M + g_\sigma\sigma) + g_\omega\omega^o + g_\rho\tau_3\rho_3^o + e\frac{1-\tau_3}{2}A^o. \tag{2}$$

Here M is the nucleon mass and σ, ω^o, ρ_3^o, and A^o are the meson and e.m. fields. These fields are to be determined self-consistently from the Klein-Gordon (KG) equations [3]; with sources (nuclear currents and densities) involving superspinors [$U(V)$] [3,4].

The RHB equations have two distinct parts: the self-consistent field (h_D) that describes the long range particle-hole correlations and the pairing field ($\hat{\Delta}$) that accounts for the correlations in the particle-particle (pp) channel. The pairing field $\hat{\Delta}$ is expressed in terms of the matrix elements of the two-body nuclear potential V^{pp} in the pp-channel and the pairing tensor involving the superspinors (U,V). In the case of the constant gap, $\hat{\Delta}_a(\equiv\Delta)$ becomes diagonal and decouples into a set of 2×2 diagonal matrices resulting in the BCS-type expressions for the occupation probabilities. As a result, the RHB equations [Eq. (1)] reduce to the RMF equations with constant gap.

Reliable and satisfactory derivation of V^{pp} is not yet available in RMF (see Refs. [3,5]). Therefore, in practical calculations, it is customary to adopt a phenomenological approach while solving the RHB equations. Usually, the finite range Gogny-D1S [6,7] interaction,

$$V(\mathbf{r}_1,\mathbf{r}_2) = \sum_{i=1,2} e^{-\{(\mathbf{r}_1-\mathbf{r}_2)/\mu_i\}^2}(W_i + B_iP^\sigma - H_iP^\tau - M_iP^\sigma P^\tau) \tag{3}$$

[factors μ_i, W_i, B_i, H_i, and M_i ($i=1,2$) are parameters of the interaction] or the density dependent, effective two-

*Electronic address: yogy@phy.iitb.ac.in

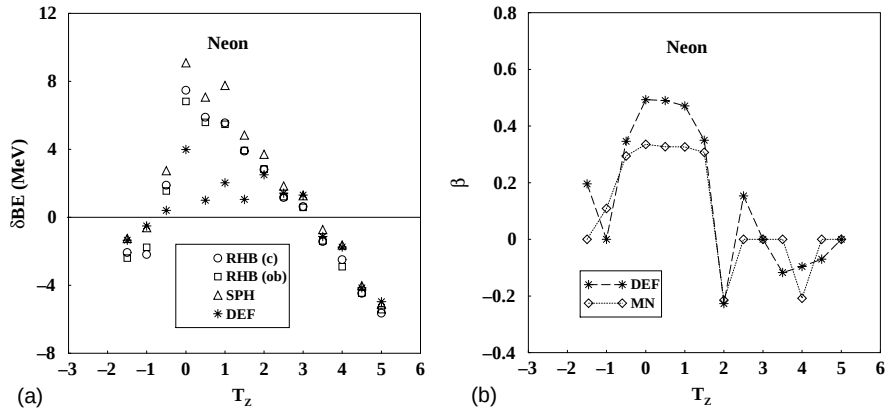

FIG. 1. (a) The binding energy differences (between the theory and the corresponding experiment [12]) as a function of the third component of isospin. (b) The calculated (DEF) and the corresponding Möller-Nix (MN) [13]quadrupole deformation parameters (β).

body zero range interaction [8],

$$V(\mathbf{r}_1, \mathbf{r}_2) = V_o \delta(\mathbf{r}_1 - \mathbf{r}_2) \frac{1}{4}(1 - \sigma_1 \sigma_2)\left(1 - \frac{\rho(r)}{\rho_o}\right) \qquad (4)$$

[V_o is the interaction strength with cutoff energy about 300 MeV [8] and ρ_o (=0.152 fm^{-3} [8]) is the nuclear matter density] are used for this purpose. In the latter case, the strength V_o is fixed so as to reproduce the pairing energy [8] obtained from the finite range Gogny D1S interaction.

The explicit calculations require (a) parameters appearing in the Lagrangian and (b) V^{pp} or the experimental gap parameters Δ (along with a cutoff, $2\hbar\omega$), as input information. Several sets of the parameters appearing in the Lagrangian are available in the literature [3,9–11]. In the present work, we use one of the recent and the most successful Lagrangian parameter set, NL3 [9].

The RMF/RHB calculations have been carried out, using different prescriptions. Explicitly, we use the following.

(1) We use the oscillator basis for the solution of (a) the RMF equations, with frozen gap approximation (corresponding results are labeled by SPH); and (b) the RHB equations using the finite range Gogny-D1S interaction [results are marked as RHB (ob)].

(2) The RHB equations are also solved on a discretized mesh in the coordinate space with a box size of 25 fm, using the effective zero range density dependent two-body interaction [8] [these results are denoted by RHB (c)].

To ascertain the effect of deformation we have also solved the RMF equations with the constant gap approximation in the axially deformed oscillator basis (the label DEF denotes these results). The constant gaps (independent of the particle level) are fixed so that the SPH pairing energy is almost same as the corresponding RHB (ob) pairing energy. The same gaps are used in the DEF calculations. For odd-A nuclei, the last odd nucleon does not have a partner to occupy its time reversed state. As a result, the mean field ground state wave function does not have time reversal symmetry. For this purpose, we follow the well tested tagged Hartree-Fock procedure, frequently used in the nonrelativistic calculations.

We now present and discuss the results of our explicit numerical calculations for the chain of neon isotopes. The differences between the calculated binding energies and the corresponding experimental values [12] are plotted in Fig. 1(a).

Clearly, all the prescriptions for solving the RMF/RHB equations reproduce the experiment rather well. However, the inclusion of deformation brings the calculated binding energies closer to the experiment. There is a discrepancy of around 4 MeV in the case of ^{20}Ne. This could be due to the possible quartet structure and/or due to the n-p pairing.

The calculated quadrupole deformation parameters (β) along with the corresponding Möller-Nix (MN) values [13] are shown in Fig. 1(b). The DEF results and MN results are very similar. The graph reveals that except for ^{18,26,30}Ne (cor-

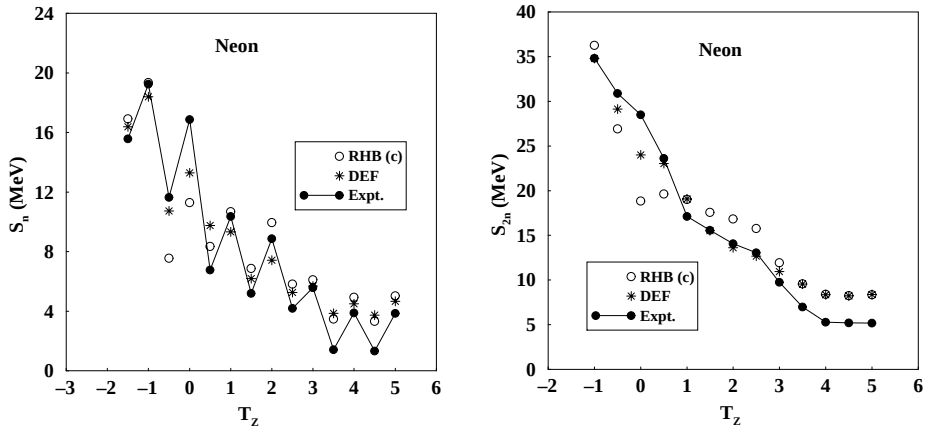

FIG. 2. The calculated [DEF and RHB (c)] single (S_n) and two neutron (S_{2n}) separation energies for the neon isotopes along with the corresponding experiment [12].

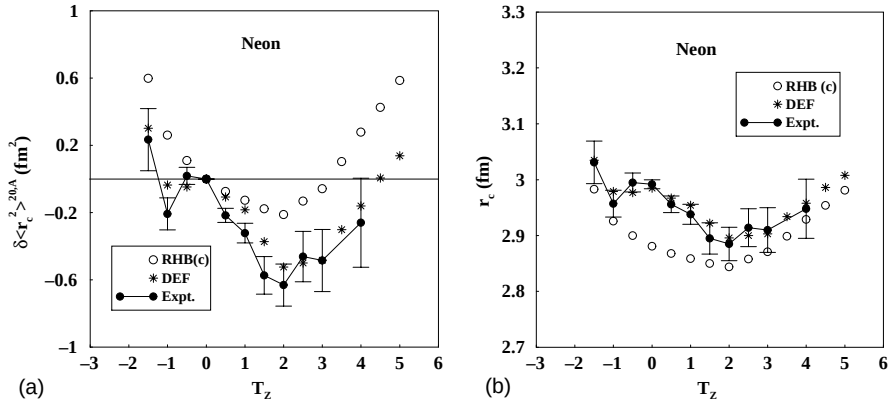

FIG. 3. The isotopic shifts (a) and the corresponding charge radii (b) for neon isotopes. The calculated values along with the corresponding experimental values [1]are shown. See text for more details.

responding to neutron numbers 8, 16, and 20, respectively), all the other neon isotopes are deformed; $^{19-23}$Ne have strong prolate deformation. The shape transition is observed between ^{23}Ne and ^{24}Ne. The higher neon isotopes have relatively milder deformations. It turns out that except for $^{20-22,28}$Ne, all the neon isotopes have very small or zero neutron pairing energies. This reflects that the deformation effects are largely due to the protons.

The RHB (c) and RHB (ob) results are almost identical and further the SPH results are similar to that of RHB (c). Therefore, we shall present and discuss the RHB (c) and DEF results only in what follows.

The variation of single and two neutron separation energies (S_n and S_{2n}) is shown in Fig. 2, with the third component of isospin T_Z, intimately related to the neutron number N [$T_Z=(N-10)/2$].

It is seen from Fig. 2 that the odd-even staggering in S_n is nicely reproduced by both RHB (c) and DEF. The inclusion of deformation effects is clearly important for the correct description of separation energies. The two neutron separation energies are also well reproduced. Differences do exist between the theory and the corresponding experiment at a finer level.

The calculated isotopic shift [$\delta\langle r_c^2\rangle$, with respect to ^{20}Ne (T_Z)=0] values [RHB (c) and DEF] along with the corresponding experimental results [1] is presented in Fig. 3(a). The DEF calculations are in excellent agreement with the experiment. The experimental trend is beautifully reproduced. In Fig. 3(b), we plot the calculated charge radii along with the corresponding values extracted from the measured isotopic shifts. The charge radius for the reference nucleus (^{20}Ne) has been taken from Ref. [14]. The calculations do reproduce the experiment. It is interesting to note that the RHB (c) underestimates the charge radii. The deformation effects are found to be crucial in order to describe the experiment correctly.

It is to be pointed out that some theoretical (both nonrelativistic and relativistic) calculations are available for this chain [15–18]. All of these have some deficiencies. The results of the nonrelativistic Hartree-Fock+BCS calculations using different types of Skyrme interactions reported in Refs. [16,17], though qualitatively similar, do differ among themselves at several places. The relativistic RMF+BCS calculations have been reported [15] for even-even neon isotopes only. The authors [15] use the Lagrangian parameter set NL3 and employ the Möller-Nix prescription for the pairing gaps [19]. The results [18] of the Skyrme Hartree-Fock+BCS and the RMF+BCS calculations for some neon isotopes have been quoted in Ref. [1].

Here, we also use the Lagrangian parameter set NL3, but fix the pairing gaps to be used in the deformed (DEF) calculations by reproducing the pairing energy obtained in RHB (ob) using Gogny-D1S interaction in *pp* channel. Though our results qualitatively agree with those of earlier calculations [15], however there are appreciable differences at several places. For example, the calculated deformation parameter β for ^{20}Ne listed in Ref. [15] is much smaller as compared to that obtained in the Skyrme Hartree-Fock+BCS calculations

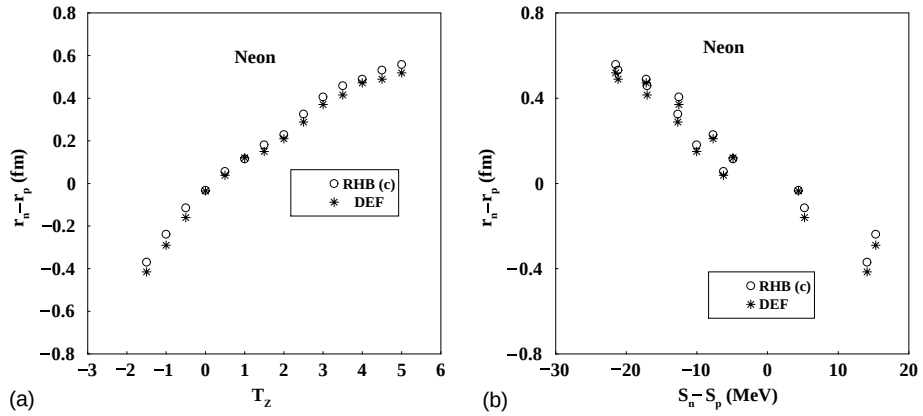

FIG. 4. The calculated [RHB (c) and DEF] nuclear skin thickness (r_n-r_p) values as (a) function of third component of isospin and (b) function of separation energy difference (S_n-S_p).

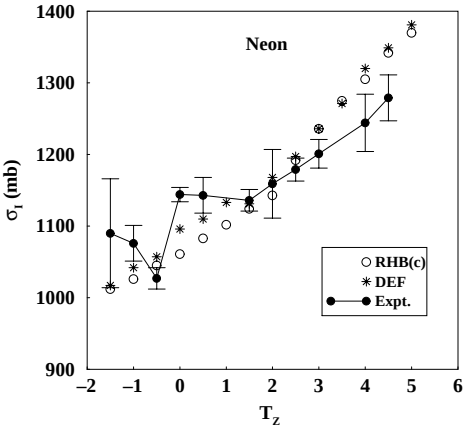

FIG. 5. The calculated [RHB (c) and DEF] interaction cross sections for neon isotopes as projectiles incident on ^{12}C target at 950 *A*MeV energy along with the experimental values [21] where available.

[16,17]. The deformation parameter β for ^{20}Ne obtained in the present work closely agrees with that of the nonrelativistic calculations [16,17] as well as with that of Möller and Nix [13]. Further, the RMF+BCS of Ref. [15] predict prolate shape for ^{24}Ne, while all the rest (nonrelativistic as well as the present calculations) yield oblate solution, which is consistent with that of Möller and Nix [13].

Overall, the results of the present calculations are in better agreement with the experiment as compared to those of RMF+BCS [15]. This indicates that proper choice of pairing gaps is important, which is expected.

The calculated nuclear skin thickness $(r_n - r_p)$ for the neon isotopes is plotted as a function of T_Z in Fig. 4(a). For ^{20}Ne, the skin is nearly zero. For the neutron deficient nuclei, the skin is negative, whereas for the neutron rich nuclei, the skin is positive as expected. The skin thickness bears nearly a linear relation with the isospin projection T_Z. Next we plot the skin thickness as a function of differences between the observed single neutron and proton separation energies $(S_n - S_p)$. A strong negative correlation is evident. To quantify the correlation, we calculate the correlation coefficient $\mathcal{C}$ defined as [20]

$$\mathcal{C} = \frac{\mathrm{Cov}(x,y)}{\sigma_x \cdot \sigma_y}, \tag{5}$$

where the covariance "Cov" is defined as

$$\mathrm{Cov}(x,y) = \frac{1}{N-1}\sum_j (x_j - \overline{x})(y_j - \overline{y}), \tag{6}$$

the variance is given by

$$\sigma_x^2 = \frac{1}{N-1}\sum_j (x_j - \overline{x})^2, \tag{7}$$

$$\sigma_y^2 = \frac{1}{N-1}\sum_j (y_j - \overline{y})^2. \tag{8}$$

The correlation coefficient $\mathcal{C}$ turns out to be -0.98 for DEF and -0.97 for RHB (c), quantifying the above statement.

The interaction cross sections for the neon isotopes as projectiles incident on ^{12}C target at 950 *A*MeV energy [21] have been measured. Here, we use the calculated [RHB (c) and DEF] densities within the Glauber Model [22] to calculate the total interaction cross section. The total interaction cross section according to the Glauber model is given by

$$\sigma_I = 2\pi \int_0^\infty b db\{1 - T(b)\}, \tag{9}$$

where b is the impact parameter and $T(b)$ is the transparency function. The calculation of $T(b)$ requires the neutron and proton densities of the target and the projectile along with the effective nucleon-nucleon cross sections. The calculated (neutron and proton) RHB (c) and DEF (renormalized projected $L=0$ component) densities are used as projectile densities whereas the target (^{12}C) density is taken from the earlier work [23]. The calculated interaction cross sections are displayed in Fig. 5 along with the corresponding experimental values [21]. Both the calculations [RHB (c) and DEF] reproduce the experimental trend well. The DEF results are relatively in better agreement with the experiment.

It is found that the inclusion of deformation effects is crucial for the correct description of the binding energies and also for the observed anomalous isotopic shifts in neon isotopes.

The authors are thankful to S. H. Patil, P. Ring, and J. Meng for their interest in this work. Partial financial support from the Department of Science and Technology (DST), Government of India (Project No. SP/S2/K-04/99) is gratefully acknowledged.

[1] W. Geithner, Ph.D dissertation, CERN-THESIS-2002-030, 14.07.2002. Available through "Geithner (search)" at the site http://cds.cern.ch/

[2] Y. K. Gambhir, P. Ring, and A. Thimet, Ann. Phys. (N.Y.) **198**, 132 (1990).

[3] P. Ring, Prog. Part. Nucl. Phys. **37**, 193 (1996), and references cited therein.

[4] W. Pöschl, D. Vretenar, and P. Ring, Comput. Phys. Commun. **103**, 217 (1997).

[5] H. Kucharek and P. Ring, Z. Phys. A **339**, 23 (1991).

[6] J. F. Berger, M. Girod, and D. Gogny, Nucl. Phys. **A428**, 32 (1984).

[7] T. Gonzalez-Llarena *et al.*, Phys. Lett. B **379**, 13 (1996).

[8] J. Meng and P. Ring, Phys. Rev. Lett. **77**, 3963 (1996); Nucl. Phys. **A635**, 3 (1998).

[9] G. A. Lalazissis, J. König, and P. Ring, Phys. Rev. C **55**, 540

(1997).
[10] P.-G. Reinhard *et al.*, Z. Phys. A **323**, 13 (1986); P. G. Reinhard, Rep. Prog. Phys. **52**, 439 (1989).
[11] M. M. Sharma, M. A. Nagarajan, and P. Ring, Phys. Lett. B **312**, 377 (1993).
[12] G. Audi and A. H. Wapstra, Nucl. Phys. **A565**, 1 (1993); Nucl. Phys. **A595**, 409 (1995); G. Audi *et al.*, *ibid.* **A624**, 1 (1997).
[13] P. Möller *et al.*, At. Data Nucl. Data Tables **59**, 185 (1995).
[14] C. W. de Jager *et al.*, At. Data Nucl. Data Tables **36**, 495 (1987).
[15] G. A. Lalazissis, S. Raman, and P. Ring, At. Data Nucl. Data Tables **71**, 1 (1999).
[16] T. Siiskonen, P. Lipas, and J. Rikovska, Phys. Rev. C **60**, 034312 (1999).
[17] S. Goriely, F. Tondeur, and J. Pearson, At. Data Nucl. Data Tables **77**, 311 (2001).
[18] P.-G. Reinhard *et al.* (unpublished), quoted in Ref. [1] as private communication.
[19] P. Möller and J. R. Nix, Nucl. Phys. **A536**, 20 (1992).
[20] D. G. Chapman and R. A. Schaufele, *Elementary Probability Models and Statistical Inference* (Xerox College Publishing, Waltham, MA, 1970).
[21] A. Ozawa, T. Suzuki, and I. Tanihata, Nucl. Phys. **A693**, 32 (2001).
[22] R. J. Glauber, *Lectures in Theoretical Physics*, edited by W. Brittin and L. Dunham (Interscience, New York, 1959), Vol. 1, p. 315.
[23] A. Bhagwat, Y. K. Gambhir, and S. H. Patil, J. Phys. G **27**, B1 (2001).